XVII ECSMGE-2019
Geotechnical Engineering foundation of the future
ISBN 978-9935-9436-1-3

doi: 10.32075/17ECSMGE-2019-0356

XVII European Conference
ECSMGE 2019 Reykjavik
on Soil Mechanics and Geotechnical Engineering

Simulation of a mini slump test using a visco-hypoplastic constitutive model in an MPM code

Simulation d'un mini test d'affaissement à l'aide d'un modèle de comportement visco-hypoplastique dans un code MPM

Martina Pippi, Claudio Tamagnini

University of Perugia, Perugia, Italy

Mario Martinelli, Dirk Luger

Deltares, Delft, The Netherlands

ABSTRACT: Tailings dams are some of the largest earth structures geotechnical engineers construct. These embankments are often built with steep slopes using the coarse fraction of the tailings thereby saving on cost. To keep such impoundments standing is one of the most challenging tasks in mine waste management. This paper presents a procedure that can be used to model the behaviour of the material stored by these dams. The constitutive model proposed by Niemunis et al. has been implemented in a UMAT subroutine with the explicit integration method proposed by Fellin & Ostermann. This model is able to describe the behaviour of soft soil because it includes the simulation of the viscous behaviour that is characteristic for these types of very soft, unstructured soils. The procedure explained in this paper is a first simulation of the behaviour of these materials through a visco-hypoplastic constitutive model implemented in a MPM code.

RÉSUMÉ: Les barrages de résidus sont l'une des plus grandes structures en terre construites par les ingénieurs géotechniciens. Ces barrages sont souvent réalisés à pente raide, et construits à base de la fraction grossière des résidus, ce qui permet de réaliser des économies. Le maintien de bassins protegés par ces digues est l'une des tâches les plus difficiles dans la gestion des déchets miniers. Cet article présente une procédure qui a pour objectif de modéliser le comportement du matériau stocké dans ces barrages. Le modèle de comportement proposé par Niemunis et al. a été implémenté dans un sous-programme UMAT employant une méthode d'intégration explicite proposée par Fellin & Ostermann. Le modèle est capable de simuler des sols mous car il prend en consideration le comportement visqueux qui caracterise ces sols non structurés. La procédure expliquée dans cet article estune première simulation du comportement de ces matériaux à travers un modèle de comportement visco-hypoplastique implémenté dans un code MPM.

Keywords: tailings dams, constitutive model, slump test.

1 INTRODUCTION

In geotechnical engineering, failure of very soft soil masses is a rather challenging problem. After failure, these kind of soils have a fluid-like behavior rather than a solid-like. Examples of such situations are given by phenomena of instability associated to the collapse of tailings dams.

Tailings dams are a particular type of dam built to store mill and waste tailings from mining activities. When the collapse of the dam occurs, the material initially stored by the dam, an extremely soft and deformable fine-grained soil, flows out downstream with extremely large displacements and deformations.

The consequences associated to these catastrophic events have a big impact on the society, and a numerical tool that can help in understanding the failure and propagation process can be used to quantify the associated risks and design possible mitigation strategies.

The modelling of tailings dams failure requires two types of improvements with respect to the current state of the art in computational geomechanics. On one hand, it is necessary to overcome the limitation inherent to the assumption of linearized kinematics adopted in small strain FE formulations, when large deformations induce severe mesh distortion. On the other hand, it is necessary to improve the description of the mechanical behaviour of the solid skeleton, by adopting a constitutive model that includes rate effects.

The contribution of this research is twofold: the behaviour of tailing muds is first described by means of a constitutive model formulated in the frame of visco-hypoplasticity; then, the constitutive model is used in a numerical code based on the Material Point Method to simulate finite deformation flow problems in such muds. To this end, a set of mini slump tests on natural muds performed at the Deltares geotechnical lab has been used to validate the proposed numerical approach.

2 NUMERICAL INTEGRATION OF THE VISCO-HYPOPLASTIC MODEL

2.1 *Visco-hypoplastic model*

The constitutive model chosen in order to simulate the behaviour of fine-grained soils characterized by low strenght and high compressibility is the visco-hypoplastic model proposed by reported by Niemunis et al. (2009). The model has been developed for normally consolidated and lightly overconsolidated clays and it is capable to describe the observed creep, relaxation, rate dependency, as well as the existence of a critical state locus under extreme deformations. Similarly to the visco-plastic approach, a preconsolidation surface (on which OCR = 1) is defined in stress space. This surface has the well-known elliptical shape of the modified Cam Clay (MCC) yield surface, but can rotate around the origin according to the evolution of an anisotropy tensor $\mathbf{\Omega}$. The preconsolidation surface is used to calculate the intensity and the direction of viscous flow. The stress point can lie outside preconsolidation surface. In this case, the distance of the current stress state from the preconsolidation surface is named “overstress” and controls the creep rate. As the overstress increases the creep rate increases, while inside the preconsolidation surface it reduces with the increase of OCR.

The evolution equation for the stress state is defined by the following constitutive laws:

$$\dot{\boldsymbol{T}} = \boldsymbol{E}\,(\boldsymbol{D} - \boldsymbol{D}^{vis} - \boldsymbol{D}^{Hp}) \tag{1a}$$
$$\boldsymbol{D}^{vis} = \boldsymbol{m} D_r (OCR)^{-1/Iv} \tag{1b}$$
$$\boldsymbol{D}^{Hp} = C_1 \boldsymbol{m}\,|\boldsymbol{D}| \tag{1c}$$

where, $\dot{\boldsymbol{T}}$ (kPa/s) is the stress rate tensor, $\boldsymbol{E}$ (kPa) is the stiffness tensor, $\boldsymbol{D}$ (1/s) is the strain rate tensor, $\boldsymbol{D}^{\mathrm{vis}}$ (1/s) is the viscous strain rate tensor, $\boldsymbol{D}^{\mathrm{Hp}}$ (1/s) is the hypoplastic strain rate tensor, $\boldsymbol{m}$ (-) is the flow rule tensor, D_{r} (1/s) is the reference strain rate and OCR (-) is overconsolidation ratio, C_1 (-) is the material constant for the hypoplastic strain and I_v (-) is the viscosity index.

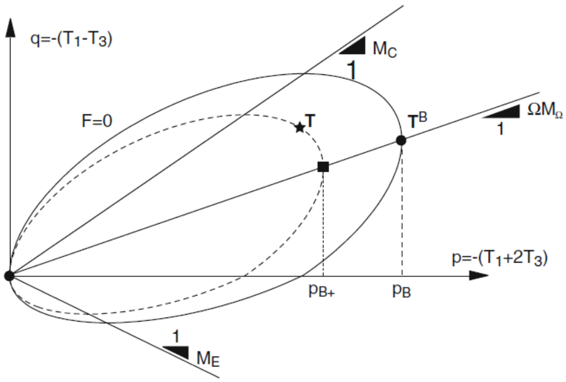

Figure 1: Anisotropic preconsolidation surface F=0 ; (Niemunis et al. 2009).

Figure 1 shows the anisotropic preconsolidation surface, its rotation is controlled by the anisotropic tensor $\mathbf{\Omega}$. The overconsolidation ratio is defined as follow:

$$OCR = \frac{p_b}{p_{b+}} \tag{2}$$

where p_b (kPa) is the preconsolidation stress and p_{b+} (kPa) the size of an ellipse homothetic to the preconsolidation surface and with the same inclination $\boldsymbol{\Omega}$, passing through the current stress point (see Fig. 1).

The model is fully characterized by the following material constants:

- e_{100} (-) Reference void ratio at 100 kPa
- λ (-) Compression index
- k (-) Swelling index
- I_v (-) Viscosity index
- D_r (1/s) Reference creep rate
- φ_c (rad) Critical state friction angle
- C_1 (-) Material constant for hypoplastic strain
- C_2 (-) Material constant controlling the evolution of the anisotropy tensor
- C_3 (-) Material anisotropy constant.

In the following, a simplified version of the model with $\boldsymbol{\Omega} = \mathbf{0}$ will be considered. Therefore, the two anisotropy coefficients C_2 and C_3 will be both set to zero.

2.2 Numerical integration

The numerical integration of the constitutive model has been done using the explicit algorithm with adptative substepping proposed by Fellin & Ostermann (2002) for the following system of ordinary differential equations:

$$\frac{d}{dt}\boldsymbol{y} = \boldsymbol{F}(\boldsymbol{y}, t) \tag{3}$$

Chosen an initial substep $0 \leq \tau \leq \Delta t$ where Δt is the given increment by the FEM/MPM code, the value for the next substep is extrapolated from the comparison between two different explicit solutions:

- Forward Euler approximation

$$\boldsymbol{v} = \boldsymbol{y_n} + \tau \boldsymbol{F_n} \tag{4}$$

- Modified Euler approximation

$$\boldsymbol{w} = \boldsymbol{y}_{\boldsymbol{n}+\frac{1}{2}} + \frac{\tau}{2}\boldsymbol{F_n} + \frac{\tau}{2}\,\boldsymbol{F}_{\boldsymbol{n}+\frac{1}{2}} \tag{5a}$$

where

$$\boldsymbol{y}_{\boldsymbol{n}+\frac{1}{2}} = \boldsymbol{y_n} + \frac{\tau}{2}\boldsymbol{F_n} \tag{5b}$$

The difference $||\boldsymbol{w} - \boldsymbol{v}|| = EST$ is an estimation of the error between the two solutions.

If the error EST is lower or equal to a user-prescribed tolerance (TOL), the solution is calculated as follows:

$$\boldsymbol{y_{n+\tau}} = 2\boldsymbol{w} - \boldsymbol{v} \tag{6a}$$

and the substep size updated according to:

$$\tau_{new} = \tau \cdot \min\left\{5; 0.9\sqrt{\frac{TOL}{EST}};\ \Delta t_{n+1} - \tau\right\} \tag{6b}$$

Conversely, if TOL > EST, the substep is rejected and τ is reduced according to:

$$\tau_{new} = \tau \cdot \max\left\{0.2; 0.9\sqrt{\frac{TOL}{EST}}\right\} \tag{7}$$

3 IMPLEMENTATION IN THE MATERIAL POINT METHOD

The material point method (MPM) can be viewed as an extension of the FEM method. In MPM, the continuum is represented by a cloud of material points that move through a computational mesh. These particles carry the physical properties of the continuum such as mass, momentum, material parameters, strains, stresses, constitutive properties and external loads.

At the beginning of each time step the information is transferred from the particles to the nodes of the computational mesh that is used to determine the incremental solution of system of governing equations. At the end of the time step the information is transferred back to the particles and the mesh is reset to the initial configuration. This process is summarized in Figure 2.

The material point method is a mesh-free method combines the best aspects of both Lagrangian and Eulerian formulations. For this reason, this method appears to be well suited to tackle engineering problems involving very large deformations.

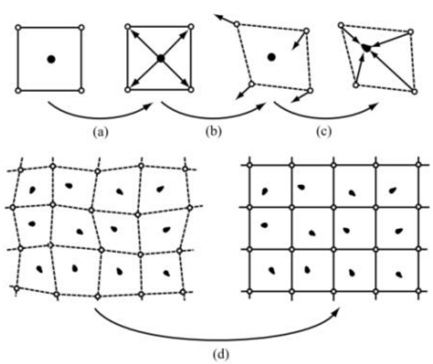

Figure 2: Schematic illustration of the MPM algorithm (Zhang, 2016).

4 MINI SLUMP TESTS

In order to validate the implementation of the constitutive model in the MPM code, some experiments named as mini slump tests have been set up.

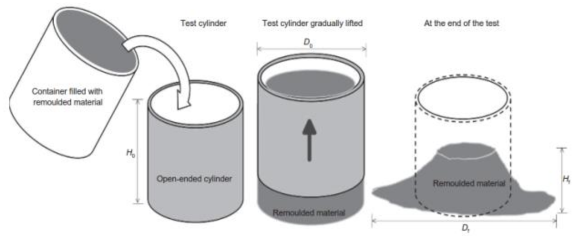

Figure 3: Description of slump test procedure ; (Thakur2014)

The mini slump test is realized filling a cylindrical container with soil and then lifting it with a prescribed velocity. The difference between the initial and the final height of the soil cylinder is the slump. This procedure is shown in Figure 3. In this study the inner diameter *D* of the cylinder was 7.8 cm. The fill height *h* inside the cylinder was varied between 0.9*D* and 1.8*D*.

The details of the complete testing program are summarized in Table 1.

Table 1. List of slump test experiments.

Test (-)	C_u **(kPa)**	h/D **(-)**	v_l **(m/s)**
1	0.117	1.8	0.06
2	0.117	0.9	0.06
3	0.117	1.8	0.01
4	0.117	0.9	0.01
5	0.072	1.8	0.06
6	0.072	0.9	0.06
7	0.072	1.8	0.01
8	0.072	0.9	0.01

Eight experiments have been performed, using a natural mud with different water contents and thus with a different undrained shear strength: C_u = 0.117 kPa for the first four tests and, after adding water to the mud, C_u = 0.072 kPa for the last four tests. Two different aspect ratios (h/D = 1.80 for the full cylinder and h/D = 0.9 for the half cylinder) and two different lifting velocities (v_l = 0.06 m/s and v_l = 0.01 m/s) have been adopted.

The experiments have been performed connecting the cylindrical container via a cable to an hydraulic plunder, which made it possible to control the lifting velocity.

The experiments have been recorded by three cameras. The shape of the mud sample has been extracted from the frames at different time intervals using an open source image processing software. Figure 4 and Figure 5 show the experimental setup.

All the surfaces in contact with the mud were covered with sand paper in order to create perfectly rough surfaces, which are far easier to model in numerical simulations than interfaces where no data on the interface strength are known.

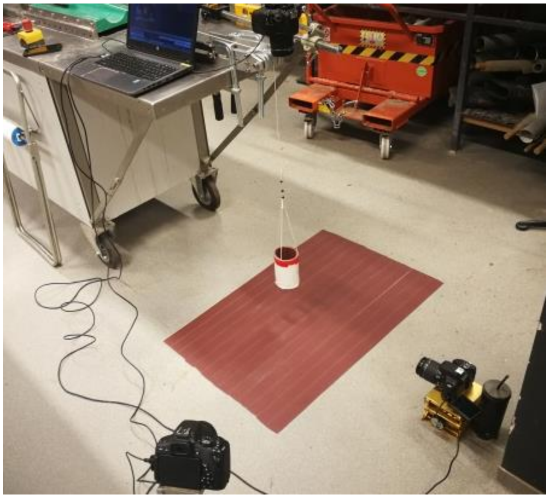

Figure 4: Video recording installation.

5 VALIDATION AND CALIBRATION OF THE MODEL

In order to validate the anisotropic visco-hypoplastic model implemented in the MPM code, the experiments described in the previous paragraph have been modelled using an axisymmetric formulation (Galavi et al., 2018).

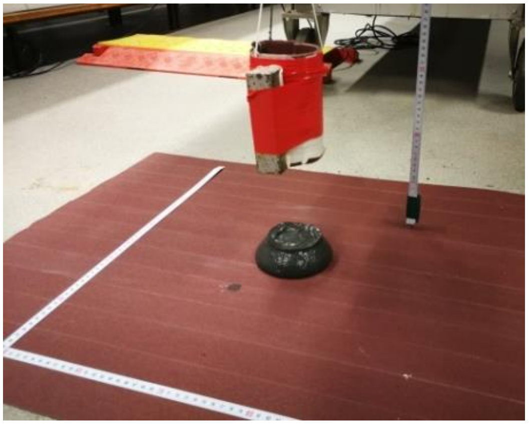

Figure 5: Slump test execution.

5.1 Geometry and materials

The geometry of the problem is shown in Figure 6, where only a cross section is simulated in 2D axisymmetric formulation.

The mesh is an unstructured mesh with quadrangular elements. The average size of each element is 0.8 cm. In each element of the mesh 4 material points are initialized. The column height is 7 cm or 14 cm, in order to reproduce the two different cases of half cylinder and full cylinder. The diameter of the cylinder is 7.8 cm, hence the radius adopted in the model is 3.9 cm. The basement is 0.5 cm thick and 0.2 m long and it is modelled with a linear elastic material.

The soil column is modelled as a visco-hypoplastic material. Undrained conditions are modelled adopting a very large bulk modulus for the water phase. No pore pressure dissipation is accounted for in the numerical model. This assumption is reasonable due to the short duration of the experiment and the very low permeability of the mud.

Since the surfaces in the test were rough, sliding was assumed to occur in the soil immediately adjacent to the surfaces, without slip at the interface itself.

For this application the cylinder container itself has not been modelled in the simulation.

The cylinder is an entity that applies a boundary condition to the lateral surface of the soil mass in the first seconds of the simulation.

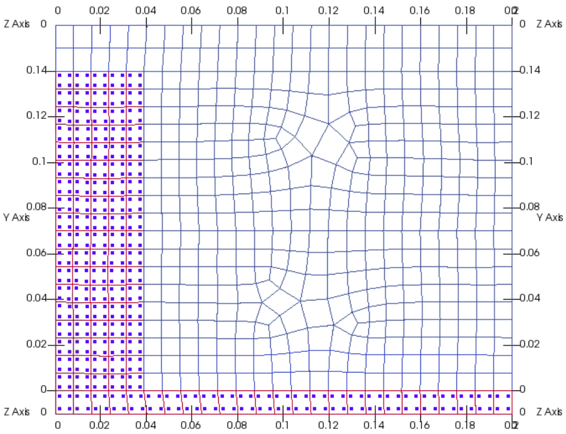

Figure 6: Geometry of the problem

5.2 *Material constants determination*

The values of e_{100}, λ, k, D_r, φ_c, have been obtained from the results of an oedometric test performed at constant strain rate, performed on the same material (Rial, 2018). In order to calibrate the remaining material constants I_v and C_1, a sensitivity analysis has been carried out by means of a series of parametric MPM simulations.

Table 2: Parameters for sensitivity analysis of I_v

e_{100} (-)	1.358
λ (-)	0.154
k (-)	0.0129
I_v (-)	0.03/0.05/0.06
D_r (m/s)	6.8e-7
φ_c (°)	14.2
C_1 (-)	0.1
C_2 , C_3 (-)	0

5.3 *Sensitivity analysis: I_v*

For the sensitivity analysis of I_v, the material constants listed in Table 2 are used. Results of the simulations are illustrated in Figure 7 for different time instants during the flow stage. The test results shown here refer to the tests with the largest lifting velocity.

The results show that I_v affects only the deformation rate in the first 20 seconds. The final deformation is the same for each of the three values.

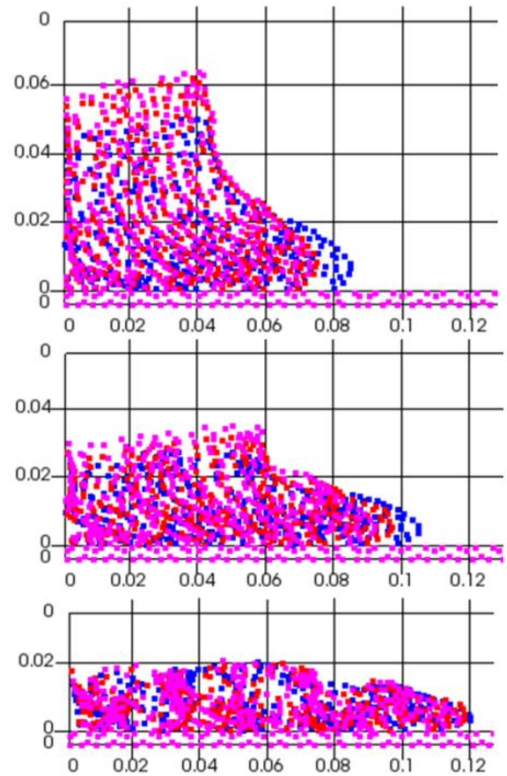

Figure 7: . Column collapse at t= 5.2/15.2/30 s; I_v = 0.03(blue)/0.05(red)/0.06(pink).

5.4 *Sensitivity analysis: C_1*

For the sensitivity analysis of C_1, the material constans listed in **Error! Reference source not found.** are used. Results of the simulations are illustrated in Figure 7 for different time instants during the flow stage.

The results show that an increase in C_1, leads to an increase of the hypoplastic strain, and therefore to a larger slump value. This is to be expected, given the constitutive equations of the model.

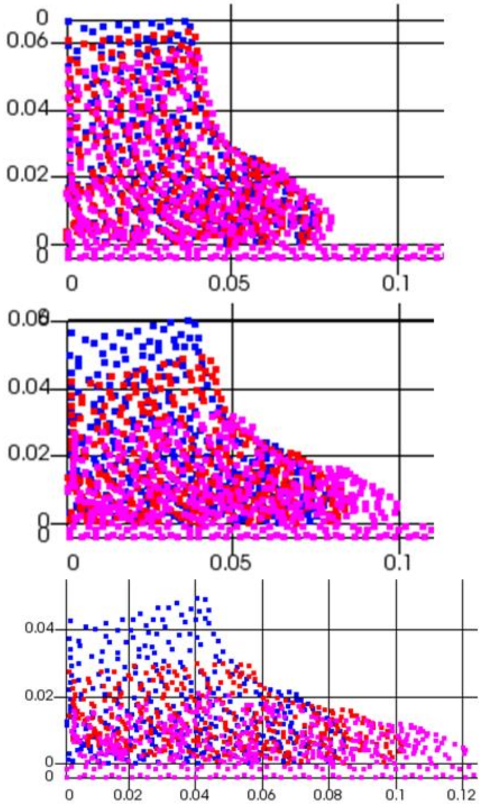

Figure 8. Column collapse at t= 4.05/ 13.3/30 s; C_1=0.025(blue)/0.05 (red)/0.1(pink).

5.5 *Final calibration*

After several numerical simulations, a final set of material constants is determined which reproduce with reasonable accuracy the observed behaviour of the material in the slump tests. This final set of material constants is reported in Tab. 4.

Table 3: Parameters for sensitivity analysis of C_1 .

e_{100} (-)	1.358
λ (-)	0.154
k (-)	0.0129
I_v (-)	0.03
D_r (m/s)	6.8e-7
φc (°)	14.2
C_1 (-)	0.025/0.05/0.1
C_2 , C_3 (-)	0

Table 4: . Parameters for final calibration.

e_{100} (-)	1.358
λ (-)	0.154
k (-)	0.0129
I_v (-)	0.02
D_r (m/s)	6.8e-7
φc (°)	14.2
C_1 (-)	0.03
C_2 , C_3 (-)	0

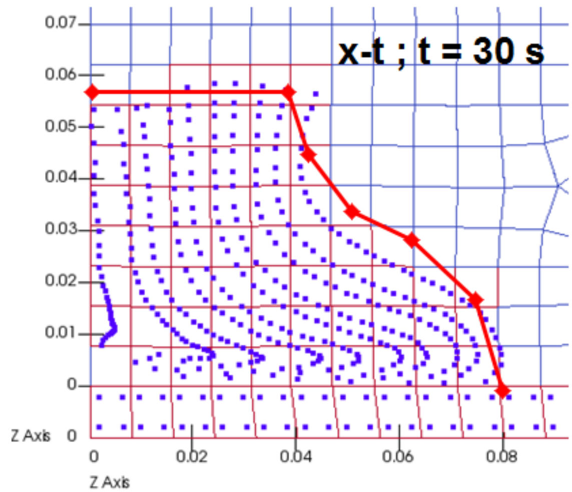

Figure 9: Comparison between the simulation (blue) and experiment (red) at t= 30 s.

Fig. Figure 9**Error! Reference source not found.** shows the comparison between the MPM simulation results and the observed soil deformation for the case with C_u = 0.117 kPa, h/D = 1.75 and lifting velocity v_l = 0.6 cm/s.

It can be observed that the measured slump profile is reproduced quite accurately by the numerical simulation.

6 CONCLUSIONS

The quite good match for the final diameter between experimental observations and the MPM predictions for this complex IBVP allows to draw the following main conclusions:

1. The visco-hypoplastic constitutive model chosen for the present work has proven to

be a good candidate for solving large deformation problems involving the flow of clay slurries or very soft clays, such as mudslides and mudflows, by means of the MPM.

2. The model has a relatively limited number of material constants, most of which are shared with the classical Modified Cam Clay model with a clear physical meaning.
3. The calibration of the material constants can be done on laboratory tests which do not need a very long duration. Automated calibration procedures, e.g. based on inverse modelling (e.g. Calvello et al, 2018; Ghasemi et al., 2018), can be set up to improve the accuracy in the calibration of non-conventional model constants, as well as to perform a back-analysis of IBVPs for which field measurements are available. The application of this procedure to the slump tests has proven to be relatively easy and computationally feasible in relatively short times.

Possible future developments of this research activitity could be an improvement of the modeling of some detailed features of the slump tests, to set-up a specific testing protocol to use these tests as a standard calibration tool for the visco-hypoplastic model and the application of the modelling procedure to simulate the run-out stage following the failure of a tailings dam.

7 ACKNOWLEDGEMENTS

The authors aknowledge Maria Barciela Rial for the technical support and for providing the mud used to perform the slump test experiments, sampled at the bottom of Markermeer lake.

8 REFERENCES

Calvello, M., Ghasemi, P., Cuomo, S., and Martinelli, M. (2018). Optimizing the MPM model of a reduced scale granular flow by inverse analysis. Proc. of 9th NUMGE Conf., Porto, Portugal

Galavi, V., Tehrani, F.S., Martinelli, M., Elkadi, A. & Luger, D. (2018) Axisymmetric formulation of the material point method for geotechnical engineering applications. Numerical Methods in Geotechnical Engineering IX – Cardoso et al. (Eds), 427-434.

Ghasemi, P., Calvello, M., Martinelli, M., Galavi, V., & Cuomo, S. (2018). MPM simulation of CPT and model calibration by inverse analysis. In Cone Penetration Testing 2018 (pp. 295-301). CRC Press.

Niemunis, A., Grandas-Tavera, C. E., & Prada-Sarmiento, L. F. (2009). Anisotropic visco-hypoplasticity. Acta Geotechnica, 4(4), 293.

Niemunis, A. (2002). Extended hypoplastic models for soils. Habilitation thesis, Ruhr University, Bochum, 2002.

Fellin W., Ostermann, A. (2002). Consistent tangent operators for constitutive rate equations. International Journal for Numerical and Analytical Methods in Geomechanics, 26:1213–1233, 2002.

Pippi, M. (2018). Numerical integration of a visco-hypoplastic constitutive model for soft clays and its implementation in a MPM code. Master of Science Thesis, University of Perugia.

Tamagnini C., Viggiani G., Chambon R. (2000). A review of two different approaches to hypoplasticity. In D. Kolymbas, editor, Constitutive modelling of granular materials, pages 107-145. Springer, 2000.

Zhang, X., Chen, Z. & Liu, Y. The material point method: a continuum-based particle method for estreme loading cases (Academic Press, 2016).

Thakur, V. & Degago, S. (2014) Quickness test approach for assessment of flow slide potentials. GEOTECHNICAL ENGINEERING 45, 85-94.

Rial, M. (2018) Private communication.